

1 Towards a Pixel TPC part II: particle identification
2 with a 32-chip GridPix detector

3 M. van Beuzekom^a, Y. Bilevych^b, K. Desch^b, S. van Doesburg^a,
4 H. van der Graaf^a, F. Hartjes^a, J. Kaminski^b, P.M. Kluit^a,
5 N. van der Kolk^a, C. Ligtenberg^a, G. Raven^a, J. Timmermans^a

6 ^a*Nikhef, Science Park 105, 1098 XG Amsterdam, The Netherlands*

7 ^b*Physikalisches Institut, University of Bonn, Nussallee 12, 53115 Bonn,*
8 *Germany*

9 **Abstract**

10 A Time Projection Chamber (TPC) module with 32 GridPixes was con-
11 structed and the performance was measured using data taken in a test beam
12 at DESY in 2021. The data analysed were taken at electron beam momenta
13 of 5 and 6 GeV/c and at magnetic fields of 0 and 1 Tesla(T). Part I of the
14 paper has described the construction, setup and tracking results.

15 The dE/dx or dN/dx resolution for electrons in the 1 T data per meter
16 of track length with 60% coverage was measured to be 3.6% for the dE/dx
17 truncation method and 2.9% for the template fit method using the successive
18 distances between the hits.

19 The single-electron efficiency at high hit rates was studied. For hit rates
20 up to 5.7 kHz per GridPix a reduction of at most 0.6% in the relative effi-
21 ciency was measured.

22 Large localized hit bursts from low energetic curling electrons were char-
23 acterised.

24 The single-electron resolution in the xy precision plane as a function of the

*Corresponding author, Telephone: +31 20 592 2000
Preprint submitted to Nuclear Instruments and Methods A
Email address: s01@nikhef.nl (P.M. Kluit)

25 local track angle ϕ was measured in the $B = 1$ T data using reconstructed
26 circular tracks. The resolution is - as expected - independent of the local
27 track angle within an uncertainty of $16 \mu\text{m}$.

28 The projected particle identification (PID) performance for a GridPix
29 Pixel TPC in the proposed ILD experiment at a future ILC e^+e^- collider
30 is presented using the $B=1$ T test beam results for the measured electron
31 PID resolution. The expected pion-kaon PID separation for momenta in the
32 range of 2.5-45 GeV/c at $\cos\theta = 0$ is more than $5.5(4.5)\sigma$ for the template
33 fit (dE/dx truncation) method.

34 *Keywords:* Micromegas, gaseous pixel detector, micro-pattern gaseous
35 detector, Timepix, GridPix, pixel time projection chamber

36 1. Introduction

37 As a step towards a Pixel Time Projection Chamber for a future col-
38 lider experiment [1], [2], a module consisting of 32 GridPixes based on the
39 Timepix3 ASIC was constructed. The GridPixes have a very fine granularity
40 of 256×256 pixels of $55 \times 55 \mu\text{m}^2$ and a high efficiency of about 85% to detect
41 single ionisation electrons.

42 The 32-GridPix chip detector was put in a test beam at DESY and com-
43 plemented with two sets of silicon detector planes. The data analysed were
44 taken at electron beam momenta of 5 and 6 GeV/c and at magnetic fields
45 of 0 and 1 T. The TPC was operated using a so-called T2K gas mixture of
46 95/3/2 gas of Ar/CF₄/iC₄H₁₀ (by volume) with a small amount of oxygen
47 and water vapour.

48 The construction of the GridPix TPC module, the test beam setup and

49 data taking conditions have been described in part I of our paper [3], that also
50 presents the track reconstruction procedure and the precise TPC tracking
51 results.

52 In the following sections, the test beam analysis results for several top-
53 ics will be presented. Firstly, the particle identification performance using
54 dE/dx or dN/dx will be measured. Secondly, the single-electron efficiency
55 at high hit rates will be determined. Thirdly, the characterisation of large
56 localized hit bursts caused by from low energetic curling electrons will be
57 presented. Fourth, the single-electron resolution in the xy precision plane
58 as a function of the local track angle will be measured. Finally, the pro-
59 jected particle identification performance for a Pixel TPC in the proposed
60 ILD experiment at ILC [4] will be presented and discussed.

61 **2. Particle Identification (PID) using dE/dx or dN/dx**

62 Particles can be identified by their characteristic energy loss per unit of
63 track length, dE/dx and/or the number of primary clusters, dN/dx produced
64 along the track. In a GridPix detector one can measure both the number of
65 hits produced along the track and their relative distance.

66 The distribution of the number of TPC track hits per GridPix for the
67 $B = 0$ T and for the $B = 1$ T data sets are a starting point for a measurement
68 of the dE/dx or dN/dx performance. As was discussed in part I of the paper
69 [3], the mean number of hits per GridPix were measured to be 124 and 89 in
70 the $B = 0$ T and 1 T data sets respectively. The most probable values are
71 respectively 87 and 64.

72 In order to measure the track performance of dE/dx or dN/dx , a track

73 selection was applied selecting tracks crossing the central chips - defined in
74 [3]. The number of hits of different GridPixes were weighted to give the same
75 mean number of hits per GridPix. By combining the hits associated to the
76 track from several events, a new 1 m long track was formed. The 1 m long
77 track has a coverage of 60% because inactive regions (chip edges and e.g.
78 guard plate) were included.

79 By applying two different analysis methods, the dE/dx or dN/dx resolu-
80 tion is measured from data.

81 Both methods project the hits along the track on the y axis - along the
82 beam direction - of the xy pixel readout plane. This gives a distribution of
83 hits as a function of the distance along the track in pixel units. The first
84 method rejects large multi-electron clusters with more than in total 6 hits in
85 5 consecutive pixel bins. Finally, a dE/dx truncation at 90% is performed
86 using samples of 20 pixels; so the 10% largest dE/dx values are removed and
87 dE/dx re-estimated. This method does not fully exploit the full granularity
88 of the pixel TPC.

89 The second method exploits the distribution of the minimum distance
90 between consecutive hits in the pixel readout plane. If only single-electron
91 clusters were produced in a gas, one would expect an exponentially falling
92 distance distribution. Multi-electron clusters will give rise to a peak at low
93 distances in the dN/dx distribution that is smeared out by the transverse
94 diffusion process. The slope of the exponential distribution is proportional
95 to the dN/dx i.e. the clusters produced by the traversing beam electron. The
96 long Landau tail in the dE/dx distribution is coming from the multi-electron
97 clusters that will peak at low distances and are smeared out by the diffusion

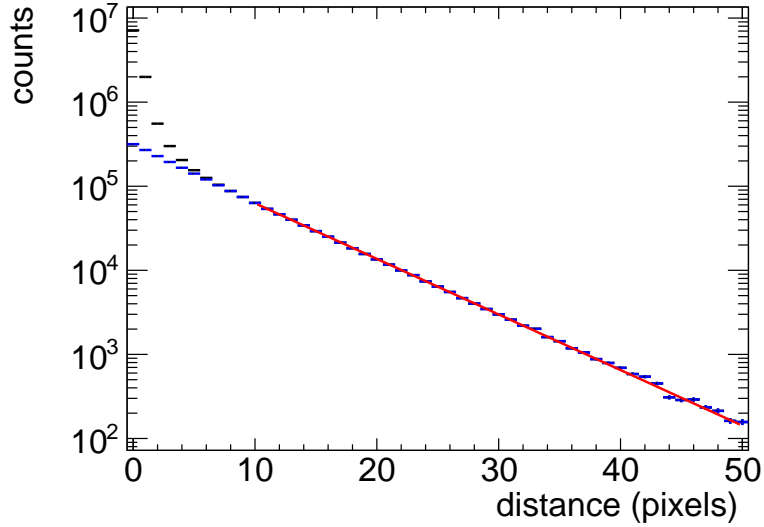


Figure 1: Distribution of the number of selected hits as a function of the distance d_y in pixel units for the $B= 1\text{T}$ data is show in black. The weighted distribution is shown with blue points and the exponential fit result with a red line.

98 proces.

99 Using a large number of tracks, it is possible to measure from data the
 100 shape of the minimum distance distribution. At distances above approx-
 101 imately 10 pixels the distribution follows an exponential distribution. At
 102 lower distance, weights for the $B= 0\text{ T}$ and 1 T data are determined and ap-
 103 plied to ensure an exponential distribution over the whole range. The values
 104 of the weights at low distances depend on the transverse diffusion coefficient
 105 and the drift length. The distribution of hits as a function of the distance
 106 d_y is shown with black points in 1 for the $B= 1\text{T}$ data. The weighted distri-
 107 bution is shown in blue and the exponential fit result - in the range of above
 108 10 pixels - with a red line.

109 Finally, per event with 1 m of track length, a maximum likelihood fit to
 110 the distance distribution in data is performed with the following template
 111 function:

$$N(d_y) = N_0 \text{weight}(d_y) e^{-\alpha \cdot d_y}, \quad (1)$$

112 where d_y is the minimum distance of the hits in the y direction of the precision
 113 plane in pixel units. The slope α and N_0 - normalisation - are left free in the
 114 per track fit. The weights for the $B = 0$ and 1 T data are fixed using the
 115 whole data set.

116 The test beam data provide a dE/dx or dN/dx measurement for electrons
 117 with a beam momentum of 5 or 6 GeV.c. The data were also used to perform
 118 a measurement of the response of a minimum ionising particle (MIP) - here
 119 defined as a particle that produced 70% of the electron dE/dx . By dropping
 120 30% of the hits associated to the track, the response of a MIP defined in terms
 121 of the number of hits (truncation method) and the fitted slope (template)
 122 was measured.

123 The relative resolution is defined as the r.m.s. of the distribution, divided
 124 by the mean and the results are shown in Table 1. The resolution of the $B =$
 125 1 T data is about 40% better than the $B = 0$ T data. This is consistent with
 126 the smaller fluctuations that are present in the distributions of the number of
 127 hits per GridPix in the $B = 1$ T data [3]. The template fit method has in the
 128 $B = 1$ T data a 20% better performance than the dE/dx truncation method.
 129 One might argue that with more diffusion the results from the template fit
 130 method will move more towards the results of the dE/dx truncation method.
 131 Note however that the diffusion contribution to the track resolution in the
 132 1 T data is already sizeable compared to the pixel size and varies between

Table 1: dE/dx or dN/dx relative resolution for different methods and data sets

Method	$B= 0$ T	$B= 1$ T
dE/dx truncation	6.0 %	3.6 %
template fit	5.4 %	2.9 %

133 85-150 μm .

134 The results for the 1 T data are shown in Fig. 2, for electrons and MIPs
 135 and for the dE/dx truncation and template fit methods. The relative error
 136 on the measured resolutions are smaller than 2.6 % and therefore neglected.
 137 The unit of the fitted slope is inverse pixel, as is clear from the formula in
 138 Eq. 1.

139 In order to estimate the performance for different particles it is important
 140 to quantify the linearity of the methods. The linearity is defined as the mean
 141 MIP response, divided by the mean electron response divided by 0.7. Clearly,
 142 one wants to use an algorithm for which the linearity is close to 1. E.g. a
 143 value of 1.2 would imply that the MIP-electron separation is 20% In our case
 144 the linearity was measured to be 1.03 for the truncation method and 1.07 for
 145 the template fit method. The statistical error on this measurement is less
 146 than 0.1 % and therefore neglected. This value is slightly different from 1.
 147 The PID performance can be corrected for by scaling the expectation values
 148 for different particles as a function of the measured momentum.

149 The dE/dx or dN/dx result of the 32-chip GridPix detector for electrons
 150 is impressive. It has currently, the best resolution per meter of track length
 151 of constructed TPCs running at atmospheric pressure - and demonstrates
 152 the particle identification (PID) capabilities of a GridPix Pixel TPC.

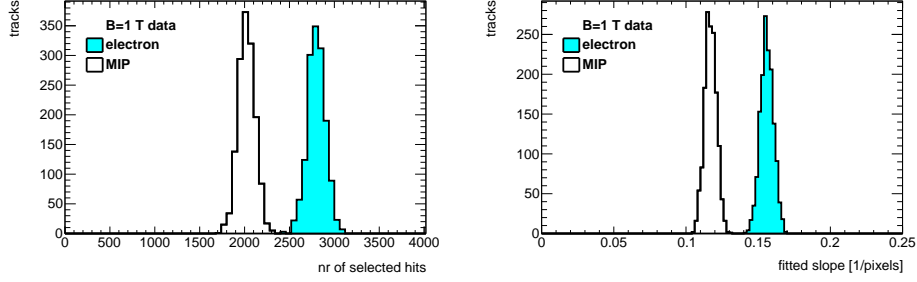


Figure 2: Distribution of the number of selected hits per track for the dE/dx truncation method (left) and the fitted slope for the template fit method (right) for an electron (light blue shaded) and for a MIP, using 1 m long tracks with 60% coverage, for the $B = 1$ T data.

153 3. Single-electron efficiency at high hit rates

154 The single-electron efficiency of the GridPix detector can be reduced in a
 155 high background environment due to the charge up of the resistive layers and
 156 the effective reduction of the amplification field. It is therefore important to
 157 measure the single-electron efficiency in different background conditions. The
 158 ToT is related to the deposited charge on the pixel and the single-electron
 159 efficiency of the detector. The relative change in the single-electron efficiency
 160 $\delta\epsilon/\epsilon$ can be related to the relative change in the mean ToT by

$$\delta\epsilon/\epsilon = d \delta\text{ToT}/\text{ToT}. \quad (2)$$

161 The derivative d is about 0.5 at the mean working point of $\text{ToT}=0.65 \mu\text{s}$ and
 162 is determined from the measured efficiency-ToT curve in Fig. 4.7 of [2]. By
 163 measuring the mean ToT in a high (low) rate environment runs at B fields
 164 of 0 and 1 T, the relative change in single-electron efficiency is extracted.

165 In order to obtain a precise result for the mean ToT, hits associated to
 166 TPC tracks were used. The track selection is the same as in section 2. The

167 analysed runs runs 6934 and 6935 and 6983 have a high hit rate and were
 168 taken at a beam momentum of 5 GeV/c. Runs 6916 and 6969 were taken
 169 at a beam momentum of 6 GeV/c and have a low hit rate. For each run
 170 the mean ToT values were measured in the interval between 0.15 and 1.4
 171 μ s. These cuts were applied to remove the noise and the upper tail of the
 172 distribution.

Table 2: Measured mean ToT and rates for different runs

run	B	ToT1	ToT2	triggers	run time	Hits1	Hits2	trig rate	Rate1	Rate2
	[T]	$[\mu$ s]	$[\mu$ s]	10^3	$[10^3$ s]	10^6	10^6	[Hz]	$[10^3$ hits/s]	$[10^3$ hits/s]
6916	0	0.628	0.653	16.8	5.81	6.25	13.1	2.9	1.08	2.26
6934	0	-	0.651	73.4	0.60	-	20.5	121.7	-	33.92
6935	0	0.620	-	73.9	0.60	6.95	-	122.5	11.51	-
6969	1	0.650	0.666	7.94	3.45	1.93	2.16	2.3	0.56	0.62
6983	1	0.657	0.678	67.9	0.70	11.6	14.1	96.2	16.44	19.94

173 The results for the measured mean ToT for different runs and hit rates are
 174 summarised in Table 2. ToT1(2) denotes the mean ToT for upper and lower
 175 half (in x) of the module and Hits1(2) corresponds to number of recorded
 176 raw hits. The number of triggers and trigger rate are not corrected for the
 177 trigger efficiency of about 31%. The mean Rate1(2) was calculated dividing
 178 the total number of raw hits by the total run time. The instantaneous rate
 179 in the high rate runs 6934, 6935 and 6983 is about a factor 3 higher (due to
 180 the duty cycle of the machine).

181 For the $B = 0$ T data, two high rate runs 6934 and 6935 taken at a
 182 beam momentum of 5 GeV/c had to be analysed because the beam crossed

183 either the upper or the lower part of the module and therefore no measure-
184 ment could be performed in one of the parts (denoted by -). The statistical
185 uncertainties are negligible.

186 The relative change in the mean ToT for the $B = 0$ data is -1.3% (upper
187 half) and -0.3% (lower half). In this case the rate goes up to 34 kHz for 6
188 chips or 5.7 kHz per GridPix. The relative change in the mean ToT for the
189 $B = 1$ T data is +1.1% (upper half) and +1.8% (lower half) The rate goes
190 up to 20 kHz for 6 chips or 3.3 kHz per GridPix.

191 Using Eq. 2, this means that the relative change in the single-electron
192 efficiency $\delta\epsilon/\epsilon$ is stable at the level of +0.9% ($B = 1$ T) and -0.6% ($B = 0$
193 T) for hit rates up to 3.3 (5.7) kHz per GridPix. To conclude, running at
194 hit rates up 5.7 kHz per GridPix gives a reduction of at most 0.6% in the
195 relative efficiency.

196 4. Characterisation of large localized hit bursts

197 In event displays large localized hit bursts from low energetic curling elec-
198 trons can be observed. An example event is shown in Fig. 3. A large variety
199 of hit patterns can be observed: large radii (open) circular tracks, smaller
200 size radius circular tracks from low momentum particles, curlers and more
201 confined bursts. A track with a momentum of 1 MeV/c will have a typical
202 radius of 60 pixels. A Pixel TPC is well suited to study and characterise these
203 typical hit bursts. After a reconstruction and characterisation of the burst it
204 is possible to reject the hits associated to the bursts. This will improve the
205 measurement of the track parameters in the final track fit.

206 To study the large localized hit bursts, the data of run 6969 - taken at a

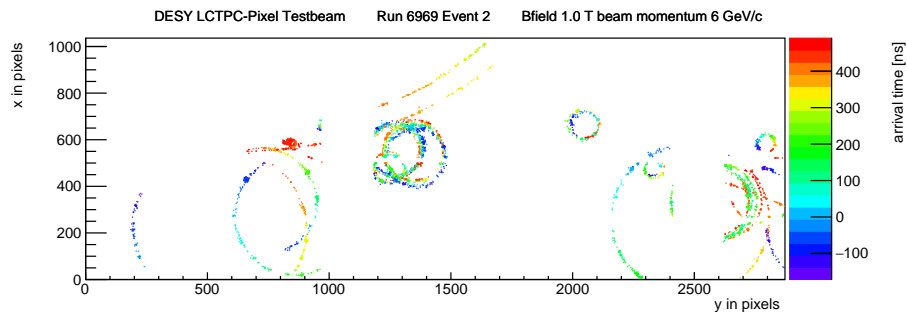


Figure 3: An event display for run 6969 event 2 taken at a 6 GeV/c beam momentum in a $B = 1$ T field. The hits are shown in the xy plane, in colour the time of arrival is shown.

207 6 GeV/c beam momentum in a $B = 1$ T field - were analysed. Bursts were
 208 selected with more than 100 hits in a radius of 50 pixels around the burst
 209 centre within a time window of 200 ns around the mean time. The mean
 210 position in xy and the mean time of the burst were iteratively estimated.
 211 The large localized hit bursts were characterised by the number of associated
 212 hits, the radius in which 90% of the hits are found (radius90) and the time
 213 in which 90% of the hits are detected (time90). The stacked distributions
 214 for the radius90 and time90 variables for different burst sizes are shown in
 215 Fig. 4.

216 It is clear that the radius90 and time90 distributions broaden as a function
 217 of the number of hits. In particular the time90 distribution develops a long
 218 tail for high number of hits. Note that hits that end up on the same pixel
 219 within the Timepix3 pixel dead time of minimally 475 ns [6] will not be
 220 recorded, so part of the core of the burst may remain undetected. The
 221 largest hit burst in the analysed run 6969 had 3180 hits.

222 For high momentum tracking it is important to cut tightly on the track

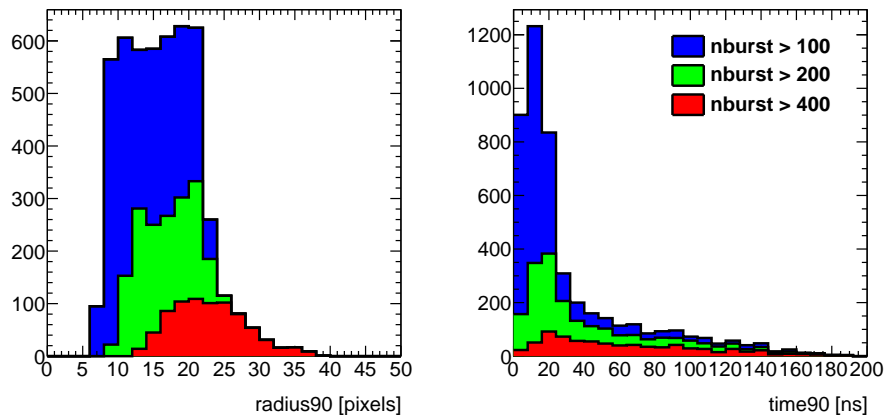


Figure 4: The stacked distributions for radius90 and time90, for large localized hit bursts with more than 100 (blue), 200 (green) and 400 (red) hits, in run 6969.

223 residuals in xy and z . In particular the cut in z reduces the impact of hit
 224 bursts in the $B = 1$ T data. Therefore in future pattern recognition software
 225 one could run a hit burst finding algorithm and down weight in the track fit
 226 the hits associated to bursts. This will remove biases and improve the track
 227 parameter estimation.

228 5. Single-electron resolution as function of the local track angle

229 The single-electron resolution in the xy precision plane as a function of
 230 the local track angle ϕ has been measured in run 6969 of the $B = 1$ T data
 231 set taken at a beam momentum of 6 GeV/c. For a pad based readout system
 232 the resolution has a strong dependence on the local track angle see e.g. [5].
 233 The resolution is the smallest if the local track angle is parallel to the strip
 234 direction.

235 For a GridPix pixel TPC - with squared pixels - the resolution is expected

236 to be independent of the local track angle. In order to test experimentally this
 237 hypothesis, reconstructed circular tracks were selected. Examples of circular
 238 tracks can be observed in the event display shown in Fig. 3. For circular
 239 tracks, the local track angle ϕ depends on the position of the individual hits
 240 on the circle in the xy plane. The range of ϕ angles depends on the radius.
 241 For radii smaller than 500 pixels a large ϕ range can be probed. Using the
 242 track residuals in the xy plane, it is possible to measure the single-electron
 243 resolution of the hits as a function of the local track angle.

244 A dedicated pattern recognition program was written to find and fit mul-
 245 tiple circular tracks in an event. To find candidate circular tracks, a Hough
 246 transform was used to find the centre of the circle in the xy plane. In the
 247 circle fit, the coarse uncertainty in xy was estimated to be about 4 pixels
 248 and in z 1 mm. Outlier hits at more than 2.5 standard deviations were it-
 249 eratively rejected. For the selection of circular tracks it was required that
 250 the fit $\chi_{xy}^2/d.o.f.$ and $\chi_z^2/d.o.f.$ were less than 5. Finally, the radius of the
 251 circle had to be larger than 50 pixels (corresponding to a momentum cut of
 252 0.8 MeV/c) and at least 20 hits should lie on the circle. The total ϕ span of
 253 the selected hits on the circle should be at least 1 rad. The hits with local ϕ
 254 values below $\pi/8$ and above $15\pi/8$ were removed due to low statistics.

255 The selected data set has 973 circular tracks, with a mean radius of 155
 256 pixels and a mean number of hits of 194. Because the resolution depends on
 257 the radius (due to the multiple scattering that increases at low momentum)
 258 and small radii span a large ϕ range, the data were re-weighted as a function
 259 of the circle radius. The weights made the momentum distribution flat as a
 260 function of the local track angle ϕ . Finally, the resolution in xy was extracted

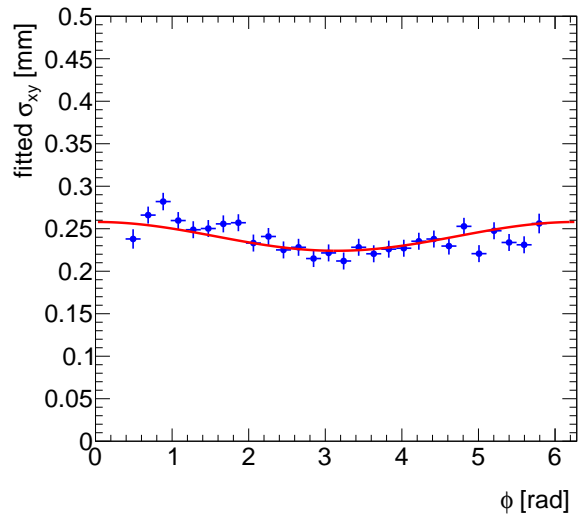


Figure 5: The fitted single-electron resolution in xy as a function of the local track angle ϕ for the hits on the circle. The fitted curve in red is given in Eq. 3.

261 - using a Gaussian fit to the track residuals in the range of $\pm 2\sigma$ around the
 262 centre. The fitted resolution in xy as a function of the local track angle ϕ
 263 for the hits on the circle is shown in Fig. 5.

264 A curve was fitted to the data using the following expression:

$$\sigma_{xy} = \sigma_0 + \sigma_1 \cos \phi, \quad (3)$$

265 where σ_0 and σ_1 were left free. The fit result yielded $\sigma_0 = 0.241$ mm and
 266 $\sigma_1 = 0.016$ mm and describes the modulation observed in the data.

267 It can therefore be concluded that the single-electron resolution in the xy
 268 precision plane is independent of the local track angle ϕ within an uncertainty
 269 of $16 \mu\text{m}$.

270 **6. Projected particle identification performance for a Pixel TPC**
 271 **in the proposed experiment ILD at a future ILC**

272 The particle identification (PID) performance of electrons in the test
 273 beam for momenta of 5-6 GeV/c was measured to be 2.9% for the tem-
 274 plate fit and 3.6% for the dE/dx truncation method at $B = 1$ T for 1 m long
 275 tracks with 60% coverage. The TPC of the proposed ILD detector [4] has
 276 an inner radius of 329 mm, an outer radius of 1770 mm and a half length of
 277 2350 mm. The electron PID resolution in the ILD TPC is expected to be
 278 2.4% (template fit) and 3% (truncation method) at polar angles of $\theta = \pi/2$
 279 ($\cos \theta = 0$) and a track length (tlength_0) of 1441 mm. The PID resolution
 280 for different particles can be written as:

$$\sigma_i = \sigma_e \sqrt{\text{tlength}_0 \cdot E_e} / \sqrt{\text{tlength} \cdot E_i}, \quad (4)$$

281 where tlength is the track length and E_i is the expected energy loss for
 282 particle i (electron = e , muon = μ , pion = π , kaon = K , proton = p).¹

283 The ILD parametrisations of dE/dx for different particles as a function of
 284 the momentum were used as given in [7]. They are based on full simulations of
 285 the ILD TPC operated with a T2K gas and running at atmospheric pressure.
 286 The PID separation in numbers of standard deviations w.r.t. the π hypothesis
 287 for e , K and p are defined as:

$$\text{PID separation}_i = |E_i - E_\pi| / \sigma_\pi. \quad (5)$$

¹Clearly, the best PID resolution will be reached for the largest track length, which corresponds to $|\cos \theta| = 0.85$ in ILD.

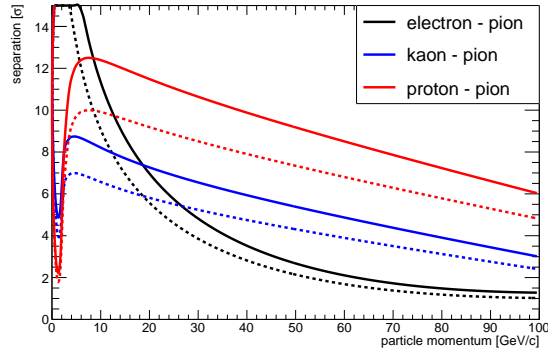


Figure 6: The projected PID separation for a GridPix TPC in ILD for electrons, kaons and protons w.r.t. pions at $\cos\theta = 0$. The continuous lines correspond to an electron PID resolution of 2.4% and the dashed to 3%.

288 In Fig. 6, the separation of electrons, kaons and protons w.r.t. pions are
 289 shown as a function of the momentum of the particle, for the projected ILD
 290 electron PID resolutions of 2.4 and 3% at $\cos\theta = 0$. The expected pion-kaon
 291 PID separation for momenta in the range of 2.5-45 GeV/c at $\cos\theta = 0$ is
 292 more than $5.5(4.5)\sigma$ for the two resolution scenarios. At a momentum of
 293 100 GeV/c the separation is still $3.0(2.0)\sigma$. Protons can be separated from
 294 pions for momenta in the range of 2.5-100 GeV/c with more than $6.0(4.8)\sigma$.

295 It is clear from the above that a GridPix Pixel TPC in ILD will provide
 296 powerful particle identification.

297 7. Conclusions and outlook

298 A Time Projection Chamber (TPC) module with 32 GridPixes was con-
 299 structed and the performance was measured using data taken in a test beam
 300 at DESY in 2021. The data analysed were taken at electron beam momenta

301 of 5 and 6 GeV/c and at magnetic fields of 0 and 1 T. The precise tracking
302 results for the module were presented in part I of the paper [3].

303 The dE/dx or dN/dx resolution for electrons with a momentum of 6
304 GeV/c in the 1 T data for a 1 m long track with 60% coverage was measured
305 to be 3.6% for the dE/dx truncation method and 2.9% for the template fit
306 method. This result is impressive and is currently the best PID resolution per
307 meter of track length of constructed TPCs running at atmospheric pressure.

308 The single-electron efficiency at high hit rates was studied. For hit rates
309 up 5.7 kHz per GridPix a reduction of at most 0.6% in the relative efficiency
310 was measured.

311 Large localized hit bursts from low energetic curling electrons were charac-
312 terised showing the pattern recognition capabilities of a GridPix Pixel TPC.

313 The single-electron resolution in the xy precision plane as a function of
314 the local track angle was measured in the $B = 1$ T data using reconstructed
315 circular tracks. It was demonstrated that the resolution in the precision plane
316 is - as expected - independent of the local track angle ϕ within an uncertainty
317 of $16 \mu\text{m}$.

318 The projected particle identification performance for a GridPix Pixel TPC
319 in ILD was presented using the $B = 1$ T test beam results for the measured
320 electron PID resolution. The expected pion-kaon PID separation for mo-
321 menta in the range of 2.5-45 GeV/c at $\cos\theta = 0$ is more than 5.5 (4.5) σ for
322 the template fit (dE/dx truncation) method.

323 It is clear that a GridPix Pixel TPC in ILD will provide powerful particle
324 identification. At the CEPC a Pixel TPC is proposed, because of the precise
325 tracking and particle identification capabilities. The GridPix detector will

326 be further tested and developed for a TPC that could be installed in a heavy
327 ion experiment at the Electron Ion Collider. In the DRD1 collaboration at
328 CERN a GridPix Pixel TPC is also part of the research program.

329 **Acknowledgments**

330 This research was funded by the Netherlands Organisation for Scientific
331 Research NWO. The authors want to thank the support of the mechanical
332 and electronics departments at Nikhef and the detector laboratory in Bonn.
333 The measurements leading to these results have been performed at the Test
334 Beam Facility at DESY Hamburg (Germany), a member of the Helmholtz
335 Association (HGF).

336 **References**

- 337 [1] M. Lupberger, Y. Bilevych, H. Blank, D. Danilov, K. Desch, A. Hamann,
338 J. Kaminski, W. Ockenfels, J. Tomtschak, S. Zigann-Wack, To-
339 ward the Pixel-TPC: Construction and Operation of a Large Area
340 GridPix Detector, IEEE Trans. Nucl. Sci. 64 (5) (2017) 1159–1167.
341 doi:10.1109/TNS.2017.2689244.
- 342 [2] C. Ligtenberg, A GridPix TPC readout for the ILD experiment at the
343 future International Linear Collider, Ph.D. thesis, Free University of
344 Amsterdam (2021). URL
345 www.nikhef.nl/pub/services/biblio/theses_pdf/thesis_C_Ligtenberg.pdf
- 346 [3] M. van Beuzekom et al., Towards a Pixel TPC part I: construction and
347 test of a 32-chip GridPix detector, Nucl. Instrum. Meth. A 1075 (2025)
348 17039. doi:10.1016/j.nima.2025.170397.

- 349 [4] T. Behnke, J. E. Brau et al., eds. The International Linear Collider.
350 Technical Design Report. Vol. 4: Detectors. Linear Collider Collabora-
351 tion, 2013. arXiv: 1306.6329. doi:10.48550/arXiv.1306.6329.
352 URL <https://www.linearcollider.org/>
- 353 [5] LCTPC Collaboration, David Attié et al., A Time Projection Cham-
354 ber with GEM-Based Readout, Nuclear Instruments and Methods in
355 Physics Research. Section A: Accelerators, Spectrometers, Detectors
356 and Associated Equipment 856, 1 (2017), 109–118. arXiv:1604.00935v1,
357 doi:10.1016/j.nima.2016.11.002.
- 358 [6] T. Poikela, J. Plosila, T. Westerlund, M. Campbell, M. De Gaspari,
359 X. Llopart, V. Gromov, R. Kluit, M. van Beuzekom, F. Zappone,
360 V. Zivkovic, C. Brezina, K. Desch, Y. Fu, A. Kruth, Timepix3: a 65K
361 channel hybrid pixel read out chip with simultaneous ToA/ToT and
362 sparse read out, JINST 9 (05) (2014) C05013.
363 URL <http://stacks.iop.org/1748-0221/9/i=05/a=C05013>
- 364 [7] iLCSoft, Linear Collider Software,
365 URL [https://github.com/iLCSoft/MarlinReco/blob/master/](https://github.com/iLCSoft/MarlinReco/blob/master/Analysis/PIDTools/)
366 [Analysis/PIDTools/](https://github.com/iLCSoft/MarlinReco/blob/master/Analysis/PIDTools/), based on version v02-02-01.